Advanced Bayesian Method for Timely Small-Scale Forest Loss Detection in the Brazilian Amazon and Cerrado with Sentinel-1 Time-Series

Marta Bottani[1,2,3,4], Laurent Ferro-Famil[2,4], Juan Doblas[5], Stéphane Mermoz[5], Alexandre Bouvet[4], Thierry Koleck[3,4]

[1] TéSA, Toulouse, 31500, France
[2] ISAE Supaero, Université de Toulouse, 31400, France
[3] Centre National d'Études Spatiales (CNES), Toulouse, 31400, France
[4] CESBIO, Université de Toulouse, CNES/CNRS/INRAE/IRD/UT3, Toulouse, 31400, France
[5] GlobEO, Toulouse, 31400, France

Keywords: Forest Loss Monitoring, Near Real-Time, Bayesian Method, Change Detection, Sentinel-1, Time Series.

Abstract

The world's forests are undergoing significant changes due to loss and degradation, emphasizing the need for Near Real-Time (NRT) monitoring to prevent further damage. Traditional monitoring methods using optical imagery are hindered by cloud coverage, while newer Synthetic Aperture Radar (SAR) systems, although operational in all weather conditions, face challenges such as sensitivity to soil moisture and the need for spatial filtering to reduce speckle effects. These limitations affect the detection of small-scale forest loss, especially in seasonally variable regions like dry forests and savannas. This paper presents a SAR-based forest disturbance detection method using Bayesian inference. Unlike traditional methods, this approach maintains the native resolution of the data by avoiding spatial filtering. Forest disturbance is modelled as a change-point detection problem within a non-filtered Sentinel-1 time series, where each new observation updates the probability of forest loss by leveraging prior information and a data model. This sequential adaptation ensures robustness against variations and trends, making it effective in monitoring disturbances across diverse forest types, including areas affected by seasonality. The proposed method was tested against other NRT monitoring systems for the year 2020, using small validation polygons (under 1 hectare) in the Brazilian Amazon and Cerrado savanna. Results demonstrate significant improvements in detecting small-scale disturbances and drastically reduced false alarm rates in both biomes. Notably, in the seasonality-sensitive Cerrado, our solution completely outperforms the leading and only existing optical technology.

1. Introduction

In recent decades, approximately 17% of moist tropical forests have vanished due to deforestation and degradation (Vancutsem et al., 2021). The capacity of forests to absorb double the CO_2 they emit underscores forests as crucial natural carbon sinks, mitigating about one-third of annual CO_2 emissions through photosynthesis (Forzieri et al., 2022). As forests diminish, global warming accelerates due to reduced CO_2 removal from the atmosphere and the release of stored CO_2 back into the air. These changes contribute significantly to biodiversity loss, impacting habitats, soil erosion, the terrestrial water cycle, and anthropogenic CO_2 emissions (Hoang and Kanemoto, 2021). Consequently, timely tools are urgently needed to monitor forest disturbances and facilitate swift interventions to support conservation efforts.

Earth Observation (EO) data offer an effective means to monitor forests across vast, often inaccessible areas. The number of EO satellites has increased substantially in recent years, along with improvements in satellite imagery quality and accessibility (Finer et al., 2018). This has led to the development of multiple operational Near Real-Time (NRT) forest disturbance detection systems. A prominent example is the Global Land Analysis and Discovery system (GLAD), initially based on Landsat imagery (GLAD-L) and later adapted to process Sentinel-2 data (GLAD-S2) (Hansen et al., 2016; Pickens et al., 2020). However, optical-based systems like GLAD face limitations due to their sensitivity to cloud cover, which is particularly problematic in tropical regions where cloud obstruction significantly reduces the amount of usable optical images, impairing timely monitoring (Verbesselt et al., 2012). As a result, recent research has shifted towards exploiting Synthetic Aperture Radar (SAR) products for forest loss detection, as SAR offers the advantage of being insensitive to clouds, ensuring a higher temporal density of time series data. The Japanese Aerospace Exploration Agency (JAXA) developed the JJ-FAST system using ALOS/PALSAR-2 SAR data, which employs multiple polarization data to detect deforestation stages based on distinct radar scattering characteristics (Watanabe et al., 2018). Such a system is limited by the 42-day revisit cycle of ALOS/PALSAR-2. Furthermore, ESA's Sentinel-1 mission, launched in 2014, has enabled the development of SAR-based systems with enhanced NRT capabilities. One such system is DETER-R by INPE in Brazil, operational in the Brazilian Amazon, using an Adaptive Linear Threshold Algorithm (ALT) for forest loss detection (Doblas et al., 2020, 2022). Another example is TropiSCO (Mermoz et al., 2021), developed by CESBIO and CNES in France, that identifies forest loss events by detecting shadows that form at the boundaries between intact forests and deforested areas (Bouvet et al., 2018; Ballère et al., 2021). The system employs moving average estimations followed by a threshold to detect sudden losses of backscatter intensity.

Nonetheless, threshold-based systems for forest loss detection (Doblas et al., 2022; Mermoz et al., 2021) often do not adequately address the complexity of forest dynamics, especially in seasonality-dependent areas where seasonal backscatter oscillations are frequently mistaken for forest loss, leading to excessive false alarm rates. As a result, seasonality-sensitive biomes are not effectively monitored by SAR technology. Furthermore, existing SAR-based systems require extensive pre-

processing, including spatial filtering to reduce speckle variations, which compromises spatial resolution and hinders the detection of small-scale disturbances such as selective logging (Carstairs et al., 2022). To address the problem's uncertainty and enhance the adaptability of forest loss detection algorithms, Bayesian approaches utilize probability to assess the likelihood of events based on available evidence. These methods enable adaptive, real-time updates of data distributions as new information becomes available, which is essential for environmental monitoring. Compared to threshold-based techniques, they offer greater flexibility and adaptability to diverse data types and complex changes (Fearnhead, 2006). Furthermore, Bayesian methods also integrate prior knowledge for improved accuracy (Adams and MacKay, 2007), and provide probabilistic measures of uncertainty in change point detection (Killick et al., 2012). In the realm of NRT forest disturbance monitoring, the RAdar for Detecting Deforestation (RADD) alerts, developed by the Laboratory of Geo-information Science and Remote Sensing at Wageningen University and Research (WUR) (Reiche et al., 2021, 2018), leverage Sentinel-1 data using a Bayesian update theory algorithm. This method assumes probability density functions for Forest (F) and Non-Forest (NF) categories, and for each new data acquisition, the NF's conditional probability is computed using Bayes' theorem, employing a block weighting mechanism to avoid certainties. The outcome is a time series of NF's conditional probabilities, which are inspected to identify potential forest loss events when surpassing a specified threshold. Pixels potentially affected by deforestation have their conditional probability of deforestation computed, with an additional threshold applied for confirmation or rejection. Similar to other SAR-based NRT forest loss detection systems, RADD employs filtering during data pre-processing to suppress speckle. Furthermore, it classifies land cover into distinct categories (F, NF) and necessitates extensive training data to define the probability distributions for each class.

In this work, we introduce a Bayesian inference-based forest disturbance monitoring technique with NRT capabilities, extendable to multiple data sources. We adapt the Bayesian Online Change Point Detection algorithm by (Adams and MacKay, 2007) to work with Sentinel-1 SAR data and enhance its capacity to detect forest loss events by considering the surrounding spatial context. Our method preserves the native spatial resolution of Sentinel-1 data by avoiding spatial filtering, and enables detection of small-scale forest loss events with an unprecedented level of accuracy. We test the method in the Amazon rainforest and the Cerrado savanna in Brazil, chosen for the availability of reliable reference data and varied vegetation types. Our validation assesses the method's effectiveness in detecting small disturbed areas using non-filtered Sentinel-1 data and its adaptability to seasonal effects in the Cerrado. Results are compared with forest loss alerts from GLAD-L (Hansen et al., 2016) and RADD (Reiche et al., 2021), and where feasible, with integrated alerts from Global Forest Watch (GFW, Retrieved in 2024).

The paper is organized as follows. Section 2 describes the input data used in this study, including details on the Sentinel-1 SAR data (Section 2.1) and a discussion of the selected study area and validation data (Section 2.2). Section 3 introduces the proposed methodology, beginning with an overview of the algorithm (Section 3.1), followed by a discussion on its implementation feasibility (Section 3.2), hints on algorithm tuning (Section 3.3), and the methodology for performance evaluation (Section 3.4). Section 4 presents the main results obtained from applying the proposed method to the validation dataset. Specifically, Section 4.1 offers a spatial comparison between the proposed method and existing operational systems for NRT forest loss monitoring. Finally, Section 5 summarizes the study's findings and offers concluding remarks.

2. Materials

2.1 Sentinel-1 Input Data

This study utilizes Sentinel-1 A/B, Interferometric Wide Swath (IW), Radiometrically Terrain Corrected (RTC) images processed by the European Space Agency (ESA). We focus on VH polarization and select either ascending or descending orbits, restricted to a single relative orbit per time series. The main features of the input data used in this work are summarized in Table 1.

The data pre-processing from Ground Range Detected (GRD) to RTC involves several steps. First, radiometric calibration is performed, converting 4.4 Equivalent Number of Looks (ENL) GRD products to calibrated intensity using gamma correction values from GRD metadata. Next, radiometric terrain correction is applied using a 30m Digital Elevation Model (DEM). Finally, the data is orthorectified to the appropriate UTM projection. We avoid further spatial filtering, preserving the original 10-meter pixel spacing of multi-looked GRD products, resulting in a ground resolution of 20 meters (azimuth) by 22 meters (range). This choice demonstrates the method's ability to maintain spatial resolution while enhancing small-scale disturbance detection.

Feature	Value
Satellite	S1A/S1B
SAR band	C band (5.405 GHz, $\lambda = 5.625$ cm)
Acquisition mode	Interferometric Wide Swath (IW)
Orbit mode	Ascending or Descending
Image product	Radiometrically Terrain Corrected (RTC)
Polarization	VH
Pixel spacing	10 m
Revisit time	6 days

Table 1. Characteristics of the Sentinel-1 input data used within the study.

2.2 Study Area and Validation Data

The experimental part of this study focuses on two areas in Brazil: the Amazon rainforest and the Cerrado woodland savanna. The Amazon, covering about 40% of Brazil's landmass, is the largest tropical forest globally and a deforestation hotspot. Monitoring this region is challenging due to constant heavy rainfall and cloud cover, which hinder optical systems (Verbesselt et al., 2012). The Cerrado, the world's most biodiverse savanna, spans over 20% of Brazil and serves as an important carbon sink. It faces rapid deforestation due to agricultural expansion, particularly for soy farming and cattle ranching (Miranda et al., 2019). Its dry and wet periods create seasonal variability in SAR signals, complicating monitoring efforts from existing NRT forest loss monitoring systems. This results in the absence of SAR-based monitoring and the low performance of optical-based monitoring in the Cerrado.

The Brazilian Amazon and Cerrado were chosen due to the availability of reliable reference data and their critical role in

global efforts to combat deforestation. According to the MapBiomas Annual Deforestation Report of 2022, over 6.5 million hectares were deforested in Brazil between 2019 and 2022, with the Amazon and Cerrado accounting for 90% of this loss. For validation, we used the MapBiomas Alerta dataset for year 2020 (MapBiomas, accessed in 2024), focusing on deforested polygons smaller than 1 hectare to demonstrate our method's effectiveness in detecting small-scale forest loss. The final validation dataset includes 629 deforested polygons in the Cerrado and 3590 in the Amazon, as shown in Figure 1.

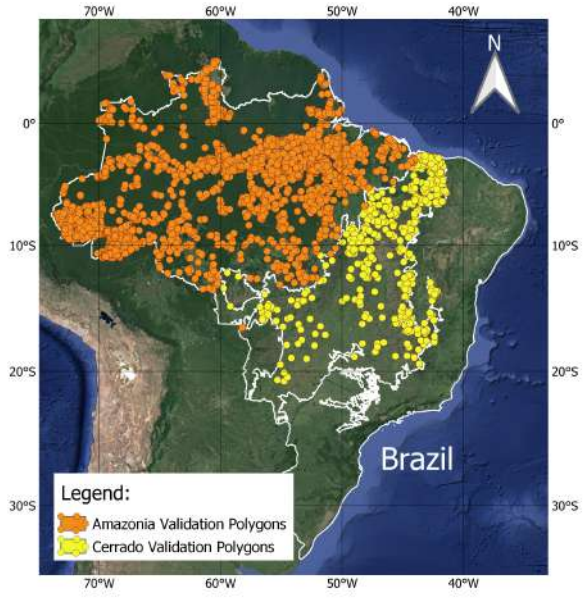

Figure 1. Map of the study area with MapBiomas Alerta validation polygons for the Amazon and Cerrado. Optical background image by Google Earth (©2024 Google).

3. Proposed Method

3.1 Bayesian Online Change Point Detection

As noted in Section 1, many existing forest disturbance monitoring systems associate forest loss with a significant drop in backscatter intensity within an affected area. However, data from C-band SAR sensors like Sentinel-1 may not exhibit such a drop due to factors like changes in soil moisture (Schmugge, 1983) or remaining vegetation (Ballère et al., 2021). To address this, our method employs Bayesian inference, which updates the probability of an event, such as forest loss, as new data becomes available. Our method, named BOCD, is based on the Bayesian Online Change Point Detection algorithm (Adams and MacKay, 2007).

In this context $\mathbf{x}_{1:t} = [x_1, \ldots, x_t]$ represents a single-pixel Sentinel-1 RTC, VH polarization, backscatter time series ordered chronologically. The algorithm assumes that the time series is segmented by change points. Its goal is to identify these change points, which mark the beginning of each new segment. The number and location of change points are determined by estimating the run length, r_t, which indicates the number of acquisitions since the last change point. The run length is a random variable associated with the hidden state of a Markov model, processed in a message-passing manner (Adams and MacKay, 2007) using observables x_t at each date. For each new acquisition, the run length can either increase by 1, corresponding to a growth phase, or reset to 0 in the case of a change point. Figure 2 shows an example of a time series along with its corresponding r_t map. The actual path associated with the time series shown on top of the figure is highlighted in black, while all potential paths of the run length are depicted in gray.

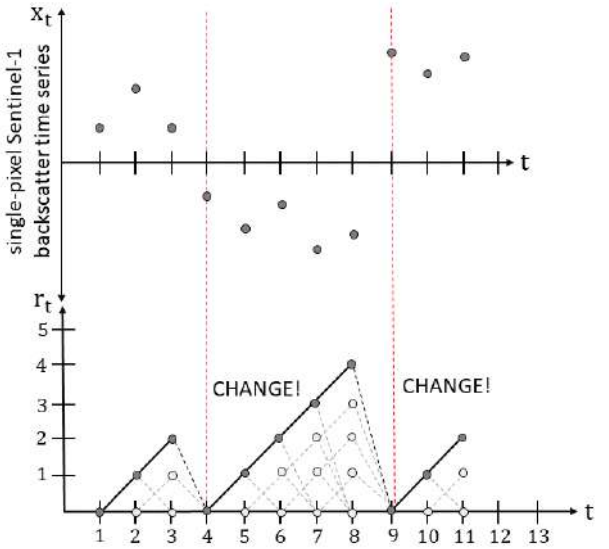

Figure 2. (**Top**) Time series showing abrupt changes marked by red dashed lines. (**Bottom**) Corresponding r_t map.

The BOCD algorithm aims at tracking the posterior probability over the run length:

$$p(r_t|\mathbf{x}_{1:t}) = \frac{p(r_t, \mathbf{x}_{1:t})}{\sum_{r_t=0}^{t} p(r_t, \mathbf{x}_{1:t})} \tag{1}$$

Such quantity is tractable if the joint distribution $p(r_t, \mathbf{x}_{1:t})$ is tractable. As detailed in (Adams and MacKay, 2007) and based on hidden Markov model properties, the joint distribution can be expressed recursively:

$$p(r_t, \mathbf{x}_{1:t}) = \sum_{r_{t-1}=0}^{t-1} p(x_t|\mathbf{x}_{t-1}^{(r_t)})\, p(r_t|r_{t-1})\, p(r_{t-1}, \mathbf{x}_{1:t-1}) \tag{2}$$

This approach enables a recursive message-passing algorithm for the posterior distribution, relying on calculating the conditional prior on the run length $r_t|r_{t-1} \sim p(r_t|r_{t-1})$, and evaluating the posterior predictive over the newly observed datum given the data since the last change point, $p(x_t|\mathbf{x}_{t-1}^{(r_t)})$. Here, $\mathbf{x}_{t-1}^{(r_t)}$ denotes a segment with run length r_t, and $p(r_{t-1}, \mathbf{x}_{1:t-1})$ represents the message. Furthermore, $p(r_t|r_{t-1})$ is designed to include contextual information within the change detection process. Assuming that within each partition, all data are modeled as independent identically distributed samples from a probability distribution with parameters governed by a prior $\theta \sim \pi(\theta)$ and a data model $x_t|\theta \sim p_\theta(x_t)$, the posterior predictive is defined as:

$$p(x_t|\mathbf{x}_{t-1}^{(r_t)}) = \int_\Theta p_\theta(x_t)\, \pi(\theta|\mathbf{x}_{t-1}^{(r_t)}) d\theta \tag{3}$$

Here, $\pi(\theta|\mathbf{x}_{t-1}^{(r_t)})$ is the Bayesian posterior over θ for the current segment, and the integral is tractable in case of conjugacy between the likelihood and the prior (Feller, 1968). The computational feasibility of the method depends on finding a closed form solution for the posterior predictive distribution, which is possible when the Bayes posterior has the same functional form as the prior. In the absence of a closed form, numerical methods are required to approximate the posterior predictive, which can be computationally expensive and unsuitable for near real-time applications.

3.2 Conjugacy and Posterior Predictive Distribution for Sentinel-1 Data

The implementation feasibility of the BOCD algorithm, as outlined in Section 3.1, hinges on whether the probability distribution of Sentinel-1 RTC data is conjugate to the prior distribution. To determine the likelihood of the Sentinel-1 data, various Probability Density Functions (PDFs) were fitted to both the backscatter intensity, I, and the logarithmic intensity data, I_{dB}, to identify the most appropriate statistical distribution. The fittings were conducted using multiple non-disturbed vegetated data samples comprising approximately 300×300 Sentinel-1 RTC pixels, collected from various locations within our study area. An example of analysis conducted for one test location is depicted in Figure 3. The goodness of fit was evaluated using the Kolmogorov-Smirnov (KS) test (Chakravarti et al., 1967). Statistical significance is achieved when the p-value is lower than a threshold α, typically set at 0.05.

The result presented in Figure 3 suggests that the I data are best represented by a log-normal distribution. Consequently, the I_{dB} data were fitted with a normal distribution using a normal-gamma conjugate prior. The closed-form solution for the posterior predictive distribution in this case is a Student's t distribution (Murphy, 2007).

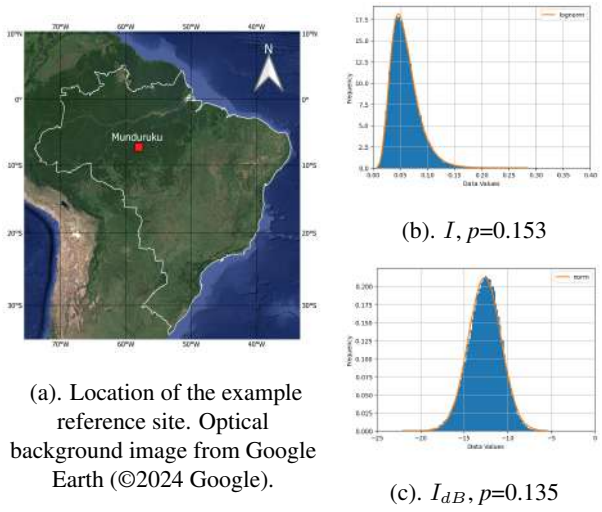

(a). Location of the example reference site. Optical background image from Google Earth (©2024 Google).

(b). I, p=0.153

(c). I_{dB}, p=0.135

Figure 3. PDF fits of I and I_{dB}, S1 RTC data (≈300×300 pixels) over an example reference site. p indicates the *p-value*.

3.3 Algorithm Tuning for Varying Conservatism in Forest Loss Detection

In the BOCD algorithm, sensitivity to change points can be adjusted by tuning the initial parameters of the posterior predictive distribution. Recalling the Student's t distribution (Murphy, 2007):

$$p(x|D) = t_{2\alpha_n}\left(x|\mu_n, \frac{\beta_n(\kappa_n+1)}{\alpha_n\kappa_n}\right) \tag{4}$$

where $D = \{x_1, ..., x_n\}$ indicates the already observed data, the distribution has four parameters: $\boldsymbol{\eta} = (\mu, \beta, \kappa, \alpha)$. A lower value of the degrees of freedom κ increases sensitivity to changes, while a higher κ makes the algorithm more conservative. The shape parameter α also affects sensitivity, with a larger α reducing sensitivity by accommodating more variability. Conversely, the mean μ and the precision β have minimal impact on sensitivity.

In Section 4, we evaluate the performance of the BOCD algorithm in the same configuration for both the Amazon and Cerrado biomes. This selected configuration represents a good balance between sensitivity and specificity.

3.4 Algorithm Performance Evaluation

The BOCD algorithm presented in Section 3.1, is applied to Sentinel-1 input data (Section 2.1). The resulting forest loss results were then validated using the MapBiomas Alerta polygons for the year 2020 as described in Section 2.2. Since the MapBiomas dataset includes deforestation polygons marked in previously forested areas, it allows the construction of a non-rigorous confusion matrix for assessing the algorithm's performance. For the 2020 monitoring year, the MapBiomas Alerta polygons (629 in the Cerrado and 3590 in Amazonia) were used to identify true positives (TP) and false negatives (FN), where a TP indicates a substantial overlap between the BOCD algorithm's output and the MapBiomas data, and a FN signifies missed forest loss events. Additionally, the 2021 MapBiomas Alerta polygons (196 in the Cerrado and 1657 in Amazonia) were used to determine false positives (FP) and true negatives (TN), where a FP represents BOCD-detected deforestation in 2020 that was not present in 2021, and a TN indicates correctly identified non-deforested areas.

The small-scale forest loss results obtained with BOCD, and compared with those from other operational forest loss monitoring systems, are presented in Section 4. In this context, the term "evaluation threshold" refers to a variable parameter used to determine if a portion of a polygon is adequate for detecting or rejecting a forest loss event.

4. Results

4.1 Spatial Comparison Between NRT Forest Loss Monitoring Systems

This section presents the 2020 forest loss detection results from the BOCD algorithm across two Brazilian biomes, comparing them with the NRT monitoring systems GLAD-L (in Amazonia and Cerrado), RADD (in Amazonia), and with GFW in Amazonia. We benchmark all comparisons against the MapBiomas Alerta dataset, which includes small-scale deforestation polygons (smaller than 1 hectare).

The confusion matrices shown in Table 2 and Table 3 compare the BOCD algorithm with other NRT forest disturbance monitoring systems in the Amazon and Cerrado biomes, respectively, in terms of percentage of true positives and false positives. The "threshold" column indicates the "evaluation threshold," which

determines the percentage of a polygon's area required to classify the entire polygon as deforested. Furthermore, the matrices report only true positives and false positives, since false negatives and true negatives can be inferred.

	True Positive TP [%]			
Threshold	BOCD	GLAD-L	RADD	GFW
75%	76.30	49.16	37.60	58.99
30%	95.93	79.22	77.49	87.27
10%	97.16	86.21	85.79	92.56
	False Positive FP [%]			
Threshold	BOCD	GLAD-L	RADD	GFW
75%	0	0.66	0.18	0.72
30%	0.30	3.80	1.45	5.43
10%	5.43	9.17	5.55	13.64

Table 2. Confusion Matrix for the Amazon Biome. TP based on MapBiomas Alerta 2020 (3590 polygons), and FP based on MapBiomas Alerta 2021 (1657 polygons).

	True Positive TP [%]	
Threshold	BOCD	GLAD-L
75%	39.90	13.35
30%	86.65	50.40
10%	95.23	61.69
	False Positive FP [%]	
Threshold	BOCD	GLAD-L
75%	0	0
30%	0.16	0.32
10%	1.11	1.75

Table 3. Confusion Matrix for the Cerrado Biome. TP based on MapBiomas Alerta 2020 (629 polygons), and FP based on MapBiomas Alerta 2021 (196 polygons).

To facilitate visual interpretation, Figure 4 illustrates the relationship between normalized true positives and normalized false positives for different evaluation thresholds across all systems. The details for Amazonia are shown in Figure 4(a), and those for the Cerrado are shown in Figure 4(b). It is important to note that the normalizations for true positives and false positives are different due to the varying total number of reference polygons, as discussed in Section 3.4. Furthermore, a good performing system is located in the top left corner of the presented graphs.

4.1.1 Amazon Biome Results Table 2 and Figure 4(a) show that RADD is more resilient to false alarms than GLAD-L, though GLAD-L shows better detection performance, especially at higher evaluation thresholds. Moreover, with BOCD, detections improve drastically over GLAD-L and RADD, especially at higher thresholds. The combined GFW system (GLAD-L + GLAD-S2 + RADD) shows superior detection performance compared to RADD and GLAD-L, though it also has more false alarms. This supports the idea that integrating SAR and optical data could enhance forest loss detection, as noted by (Doblas et al., 2023); this line of work will be explored further in the future. Overall, we highlight the increased resilience of BOCD to false alarms in comparison to other systems.

4.1.2 Cerrado Biome Results Table 3 and Figure 4(b) show the relationship between normalized true positives and normalized false positives for various evaluation thresholds in the Cerrado. The comparison is limited to GLAD-L, as RADD and GLAD-S2 are not operational in this area, leading to most GFW alerts being low confidence and excluded from this research.

The results consistently demonstrate that BOCD outperform GLAD-L in both detections and false alarm reduction. Specifically, BOCD's true positives are nearly double those of GLAD-L, especially at high evaluation thresholds.

To the authors' knowledge, there is no SAR-based NRT forest loss monitoring system currently operational in tropical savannas, making the results just presented a key contribution of our work.

4.1.3 Comparing Overestimation of Small-Scale Deforestation by Existing Systems with BOCD Figure 5 highlights the tendency of existing NRT forest disturbance monitoring systems to overestimate small-scale deforestation events. These systems often struggle with detecting small disturbances accurately, due to their reliance on spatial filtering techniques in the pre-processing of the data stack. Spatial filtering, while effective at reducing speckle variations in SAR images, can also lead to a decrease in spatial resolution and, consequently, to an overestimation of small-scale deforestation.

In contrast, the BOCD algorithm demonstrates superior detection capabilities for small-scale deforestation activities. This is achieved by using the non-spatially filtered Sentinel-1 RTC data time-series, which preserve the native spatial resolution and allow for more accurate detection of subtle forest loss events.

5. Conclusions

In this study, we present a novel, unsupervised, Sentinel-1-based method for near real-time forest disturbance detection using Bayesian inference. Building on the framework developed by (Adams and MacKay, 2007), we adapted this methodology to include spatial context by considering the proximity to previously observed deforestation events. Moreover, our method preserves measurement resolution by avoiding spatial filtering as a pre-processing step, thereby enhancing the detection of small-scale forest loss.

We applied the BOCD algorithm to monitor forest loss in the Brazilian Amazon and Cerrado woodland savanna throughout 2020. For validation, we utilized the MapBiomas Alerta dataset, focusing on small-scale deforestation polygons (i.e., $<$1 ha) for 2020 to evaluate detections and omissions, and for 2021 to assess false alarms and true negatives. Our results were compared against alerts from other operational NRT systems, including GLAD-L for both Amazonia and Cerrado, as well as RADD and GFW for Amazonia.

The analysis demonstrated that BOCD surpassed all other systems in terms of detection capabilities while maintaining a relatively low false alarm rate. Furthermore, our focused comparison revealed that existing systems tend to overestimate deforestation due to spatial filtering effects, whereas BOCD achieved more accurate detections across various evaluation thresholds.

In conclusion, our adaptive BOCD approach significantly improves small-scale forest loss detection with low false alarm rates, making it a valuable tool for monitoring both the Amazon and the dynamic carbon sink region of the Cerrado, where existing systems face limitations or are entirely absent.

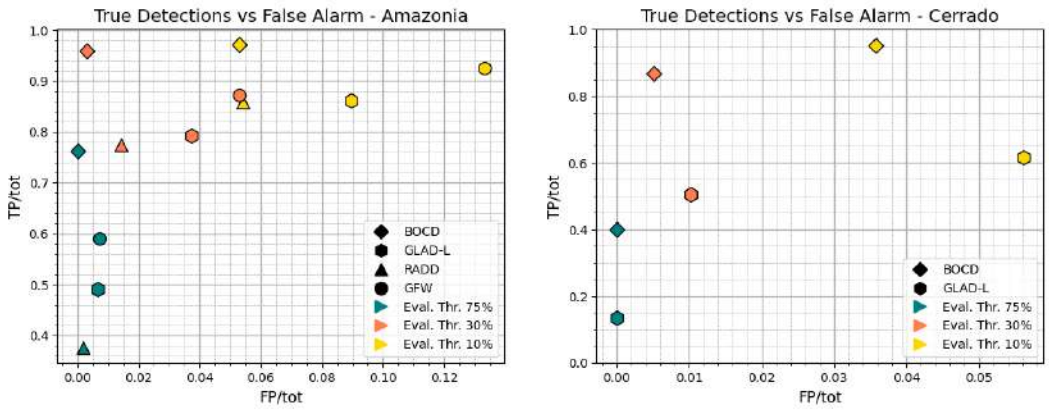

(a). Amazon biome.

(b). Cerrado biome.

Figure 4. Comparison of normalized true positives and false positives across different systems, with colors representing various evaluation thresholds.

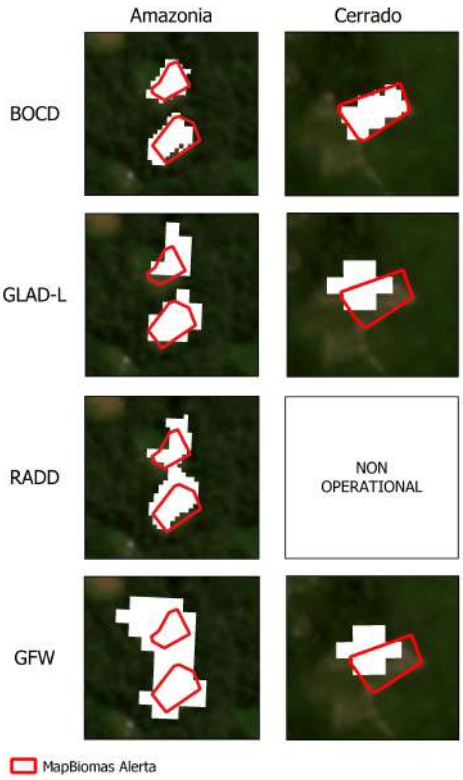

Figure 5. Comparison of spatial precision between BOCD and existing NRT forest loss monitoring systems on two example polygons.

Acknowledgements

Marta Bottani's research was supported by the Centre National d'Études Spatiales (CNES) and ISAE Supaero, and hosted by the TéSA and CESBIO laboratories in Toulouse, France. This study has been partially supported through the grant EUR TESS N°ANR-18-EURE-0018 in the framework of the Programme des Investissements d'Avenir, as well as by ISAE Supaero and GdR IASIS mobility grants. Finally, the authors would like to thank the Universidade Federal do Pará (UFPA) for welcoming Marta Bottani on their campus for a valuable and stimulating exchange experience.

References

Adams, R. P., MacKay, D. J., 2007. Bayesian online changepoint detection.

Ballère, M., Bouvet, A., Mermoz, S., Toan, T. L., Koleck, T., Bedeau, C., André, M., Forestier, E., Frison, P.-L., Lardeux, C., 2021. SAR data for tropical forest disturbance alerts in French Guiana: Benefit over optical imagery. *Remote Sensing of Environment*, 252, 112159.

Bouvet, A., Mermoz, S., Ballère, M., Koleck, T., Toan, T. L., 2018. Use of the SAR Shadowing Effect for Deforestation Detection with Sentinel-1 Time Series. *Remote Sensing*, 10(8).

Carstairs, H., Mitchard, E. T. A., McNicol, I., Aquino, C., Chezeaux, E., Ebanega, M. O., Dikongo, A. M., Disney, M., 2022. Sentinel-1 Shadows Used to Quantify Canopy Loss from Selective Logging in Gabon. *Remote Sensing*, 14(17).

Chakravarti, I., Laha, R., Roy, J., 1967. *Handbook of Methods of Applied Statistics, Volume I*. Wiley, 392–394.

Doblas, J., Lima, L., Mermoz, S., Bouvet, A., Reiche, J., Watanabe, M., Anna, S. S., Shimabukuro, Y., 2023. Intercomparison of optical and SAR-based forest disturbance warning systems in the Amazon shows the potential of combined SAR-optical monitoring. *International Journal of Remote Sensing*, 44(1), 59-77.

Doblas, J., Reis, M. S., Belluzzo, A. P., Quadros, C. B., Moraes, D. R. V., Almeida, C. A., Maurano, L. E. P., Carvalho, A. F. A., Sant'Anna, S. J. S., Shimabukuro, Y. E., 2022. DETER-R: An Operational Near-Real Time Tropical Forest Disturbance Warning System Based on Sentinel-1 Time Series Analysis. *Remote Sensing*, 14(15).

Doblas, J., Shimabukuro, Y., Sant'Anna, S., Carneiro, A., Aragão, L., Almeida, C., 2020. Optimizing near real-time detection of deforestation on tropical rainforests using Sentinel-1 data. *Remote Sensing*, 12(23).

Fearnhead, P., 2006. Exact and efficient Bayesian inference for multiple changepoint. *Statistics and Computing*, 16(2), 203-213.

Feller, W., 1968. *An Introduction to Probability Theory and Its Applications: Volume I*. Wiley.

Finer, M., Novoa, S., Weisse, M. J., Petersen, R., Mascaro, J., Souto, T., Stearns, F., Martinez, R. G., 2018. Combating deforestation: From satellite to intervention. *Science*, 360, 1303-1305.

Forzieri, G., Dakos, V., McDowell, N. G., Ramdane, A., Cescatti, A., 2022. Emerging signals of declining forest resilience under climate change. *Nature*, 608, 534–539.

GFW, Retrieved in 2024. World resources institute - global forest watch. `https://data.globalforestwatch.org/datasets/gfw::integrated-deforestation-alerts/about`.

Hansen, M. C., Krylov, A., Tyukavina, A., Potapov, P. V., Turubanova, S., Zutta, B., Ifo, S., Margono, B., Stolle, F., Moore, R., 2016. Humid tropical forest disturbance alerts using Landsat data. *Environmental Research Letters*, 11(3), 034008.

Hoang, N. T., Kanemoto, K., 2021. Mapping the deforestation footprint of nations reveals growing threat to tropical forests. *Nature Ecology and Evolution*, 5, 845–853.

Killick, R., Fearnhead, P., Eckley, I. A., 2012. Optimal Detection of Changepoints With a Linear Computational Cost. *Journal of the American Statistical Association*, 107(500), 1590-1598.

MapBiomas, accessed in 2024. Mapbiomas alert project - validation and refinement system for deforestation alerts with high-resolution images. `https://alerta.mapbiomas.org/en`.

Mermoz, S., Bouvet, A., Koleck, T., Ballère, M., Toan, T. L., 2021. Continuous Detection of Forest Loss in Vietnam, Laos, and Cambodia Using Sentinel-1 Data. *Remote Sensing*, 13(23).

Miranda, J., Börner, J. J., Kalkuhl, M., Soares-Filho, B. S., 2019. Land speculation and conservation policy leakage in Brazil. *Environmental Research Letters*, 14.

Murphy, K. P., 2007. Conjugate bayesian analysis of the gaussian distribution. Technical report, The Univeristy of British Columbia.

Pickens, A. H., Hansen, M. C., Adusei, B., P.Potapov, 2020. Sentinel-2 forest loss alert. global land analysis and discovery (glad). Accessed through Global Forest Watch.

Reiche, J., Hamunyela, E., Verbesselt, J., Hoekman, D., Herold, M., 2018. Improving near-real time deforestation monitoring in tropical dry forests by combining dense Sentinel-1 time series with Landsat and ALOS-2 PALSAR-2. *Remote Sensing of Environment*, 204(5), 147-161.

Reiche, J., Mullissa, A., Slagter, B., Gou, Y., Tsendbazar, N.-E., Odongo-Braun, C., Vollrath, A., Weisse, M. J., Stolle, F., Pickens, A., Donchyts, G., Clinton, N., Gorelick, N., Herold, M., 2021. Forest disturbance alerts for the Congo Basin using Sentinel-1. *Environmental Research Letters*, 16(2), 024005.

Schmugge, T. J., 1983. Remote Sensing of Soil Moisture: Recent Advances. *IEEE Transactions on Geoscience and Remote Sensing*, GE-21, 336-344.

Vancutsem, C., Achard, F., Pekel, J.-F., Vieilledent, G., Carboni, S., Simonetti, D., Gallego, J., Aragão, L. E., Nasi, R., 2021. Long-term (1990–2019) monitoring of forest cover changes in the humid tropics. *Science Advances*, 7.

Verbesselt, J., Zeileis, A., Herold, M., 2012. Near real-time disturbance detection using satellite image time series. *Remote Sensing of Environment*, 123, 98-108.

Watanabe, M., Koyama, C. N., Hayashi, M., Nagatani, I., Shimada, M., 2018. Early-stage deforestation detection in the tropics with L-band SAR. *IEEE Journal of Selected Topics in Applied Earth Observations and Remote Sensing*, 11, 2127-2133.